STEEL-PLATE COMPOSITE (SC) WALLS: ANALYSIS AND DESIGN INCLUDING THERMAL EFFECTS

Amit H. Varma[1], Sanjeev R. Malushte[2], Kadir C. Sener[3], Peter N. Booth[4] , Keith Coogler[5]
[1]Assoc. Professor, Bowen Lab., School of Civil Eng. Purdue Univ., W. Lafayette, IN. ahvarma@purdue.edu
[2]Bechtel Fellow and Sr. Principal. Engineer, Bechtel Power Corp., Frederick, MD. smalusht@bechtel.com
[3]Ph.D. Cand., Bowen Lab., School of Civil Eng. Purdue Univ., W. Lafayette, IN. ksener@purdue.edu
[4]Ph.D. Cand., Bowen Lab., School of Civil Eng. Purdue Univ., W. Lafayette, IN. boothpn@purdue.edu
[5]Senior Engineer, Westinghouse Electric Company, Cranberry Township, PA. cooglerkl@westinghouse.com

ABSTRACT

Steel-plate composite (SC) walls are of significant interest for designing containment internal structures for third generation nuclear power plants. As part of containment internal structures, these walls may be exposed to combined thermal and mechanical loading in the event of a postulated accident scenario. The performance of SC walls subjected to combined thermal and mechanical loading is of concern because, as opposed to rebar in reinforced concrete walls, the steel faceplates of SC structures are directly exposed to the thermal loading. This paper summarizes the results of experimental and analytical evaluation of the effects of combined thermal and mechanical loading on the behavior of SC walls. These evaluations indicate that SC walls subjected to accident thermal loading develop nonlinear temperature gradients through the wall thickness and undergo concrete cracking. This concrete cracking significantly reduces the stiffness of the SC walls, and thus the thermally induced forces and moments. The paper includes recommendations for: (i) estimating the structural stiffness of SC walls subjected to accident thermal loading, (ii) estimating the maximum moments induced due to thermal gradients, and (iii) developing linear elastic finite element (LEFE) models of SC walls for conducting dynamic seismic analysis.

INTRODUCTION

Steel-plate composite (SC) walls are being considered for the containment internal structures (CIS) in third generation nuclear power plants. SC wall construction allows for shortened construction schedules since modules can be prefabricated away from the construction site and then shipped and rapidly erected [1]. Modular SC designs have also demonstrated adequate structural performance and ductility during extreme loading if detailed properly [2]. The cost savings of SC modular construction compared to reinforced concrete are beginning to become evident from current power plant construction projects that have successfully implemented SC modular construction.

This paper summarizes results from an ongoing multi-year project at Purdue University, Bowen Laboratory studying the behavior of SC walls subjected to simultaneous thermal and mechanical loading. The results from a previous testing program [3, 4, 5] are combined with the results from additional tests, thus adding to the overall body of experimental testing knowledge. Within the context of CIS, these SC walls may be exposed to a simultaneous combination of thermal and mechanical loads in the event of a postulated accident scenario. Unlike reinforced concrete which has a protective layer of concrete cover, SC walls have steel plates on the inner and outer surfaces that can be directly exposed to thermal loads.

The objectives of this paper are: (i) to expand upon previous analytical and experimental research, and (ii) provide recommendations for analysis and design of SC walls subjected to combined thermal and mechanical loads.

DESCRIPTION OF SPECIMENS, TEST SETUP AND LOADING PROTOCOL

The authors have previously [3, 4, 5] tested two full-scale 22-ft long SC beam specimens designed to represent the (essentially one-way) behavior of horizontal segments of a modular SC wall panel away from the horizontal boundary conditions. Each beam specimen had a depth of 31 in., width of 30 in., and consisted of two 0.5 in. thick A572 Gr. 50 steel faceplates. These faceplates were connected to each other by steel channels that were spaced at 30 in. and welded to the plate surfaces. Additionally, 3/4 in. diameter, 6 in. long Nelson shear studs were welded to the inner steel faces and spaced on a 10 x 10 in. orthogonal layout, These shear studs anchored the steel faceplates to the 5000 psi compressive strength concrete infill. Some details of the specimens are shown in Figure 1.

The beam specimens were configured in a typical four point bending test setup with simple supports at both ends and concentrated forces applied at two load points that were 8 ft. from the supports using 100 kip capacity actuators. Thus, the middle 6 ft of the span was subjected to uniform moment, and the 8 ft. spans close to the supports were subjected to uniform shear. The shear span-to-depth (a/d) ratio for the specimens was 3.2.

The effects of thermal loading (heating) on the flexural and shear behavior of SC beams was investigated using two specimens. Specimen 1 was subjected to heating in the uniform moment region (central 6 ft.) of the span.

It was used to investigate the effects of thermal loading on the flexural behavior and stiffness. Specimen 2 was subjected to heating in the shear span where the heating length was equal to 6 ft and centered around one of the loading points. It was used to investigate the effects on thermal loading on the shear behavior and strength

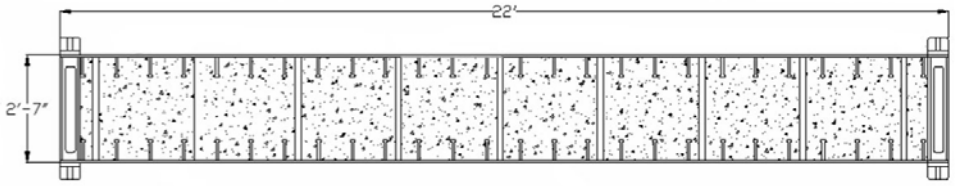

Fig. 1: Dimensions and Detailing of Specimen 1 and 2

Specimens 1 and 2 were initially subjected to loading such that the bending moment in the uniform moment region was approximately equal to that produced by an equivalent pressure of 10 psi acting on the SC wall. The magnitude of this loading was equal to 25 kips. After loading, the specimens were subjected to heating (simulating thermal loading effects). The top steel faceplates were heated (over the lengths mentioned above and discussed in detail in [3]) from ambient to 300^{o}F in less than 15 minutes. The steel faceplate temperature was maintained at 300^{o}F for 2 hours. After two hours of heating, the applied loading was increased monotonically to 90 kips, which is equivalent to pressure loading of 36 psi on the SC wall, and thus an over strength factor of approximately 3.6. Neither of the Specimens 1 or 2 had failed at the load level of 90 kips.

The authors have recently tested another SC beam specimen (Specimen 3). The objective of testing Specimen 3 was to further verify the results from the experimental and analytical investigations conducted earlier [presented in 3, 4, and 5], and to address some limitations of the earlier research. The major limitation was that the specimens could not be loaded to failure due to the capacity limit of the loading frame setup. As a result, the effects of thermal cracking on the out-of-plane failure strength of the SC beam specimens could not be ascertained.

Specimen 3 was similar to the earlier two specimens, with the exception that the channel spacing was increased to 48 in. (1.6 times section depth). Some details of Specimen 3 are shown in Figure 2. As shown the specimen was 30 in. wide and 30 in. deep. It was 24 ft long with simple supports and two concentrated load points. The uniform moment region was 4 ft. long, and the shear spans (a) were 8ft 9in. long, resulting in a/d ratio of 3.5.

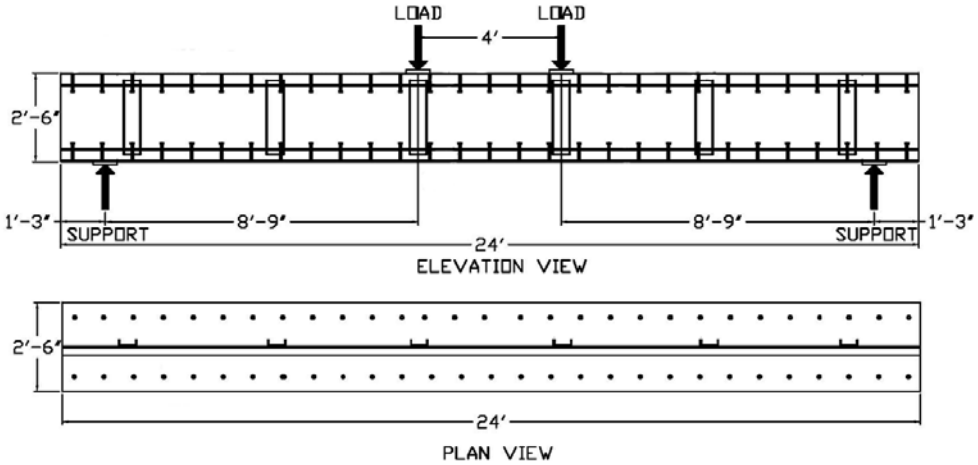

Fig. 2: Dimensions and Load Configuration of Specimen 3

Specimen 3 was initially subjected to loading such that the bending moment in the uniform moment region was approximately equal to that produced by an equivalent pressure of 20 psi acting on the SC wall. The magnitude of this loading was equal to 40 kips. The setup for applying thermal loading is shown in Figures 3 and 4. As shown, four electrical heater panels (described in detail in [3]) were suspended above the top steel faceplate. The heaters were located adjacent to the load point in the shear span so that the portion of the beam with maximum moment and shear would be exposed to the thermal loading. The heaters were controlled to increase the steel faceplate temperature from ambient to 300^{o}F in approximately 10 minutes. The steel faceplate temperature was maintained at 300^{o}F for about 3 hours, after which the mechanical loading was increased to failure. The steel faceplate was maintained even while increasing the mechanical loading to failure. The experimental results presented in this paper

focus on Specimen 3 since it was loaded to failure and provided more comprehensive data to evaluate the effects of accident thermal loading on the out-of-plane behavior of SC walls.

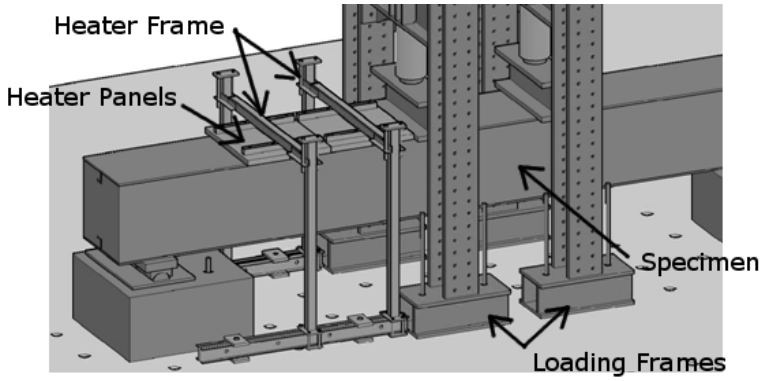

Fig. 3: Four Point Load Test Setup with Heater Panels

Fig. 4: Heater Test Setup over Shear Span

EXPERIMENTAL BEHAVIOR

Figure 5 shows the temperatures measured on the steel surface and on the channel in the center of the heated region of Specimen 3. It shows the transient temperatures measured through the thickness of the cross-section including at the heated steel surface, and 2, 4, 7, and 12 in. below the heated surface. As shown, the steel plate reaches its elevated temperature 300°F (148°C) almost immediately. The temperature increases are much smaller and much slower for locations within the depth of the section. There is almost no change in temperature for locations 7 in. and deeper within the section. This figure also illustrates the steep nonlinear temperature gradient that develops through the cross-section because of thermal loading on only one steel faceplate.

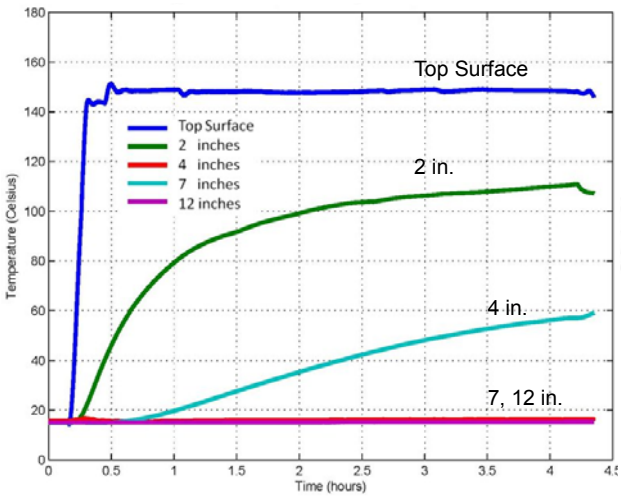

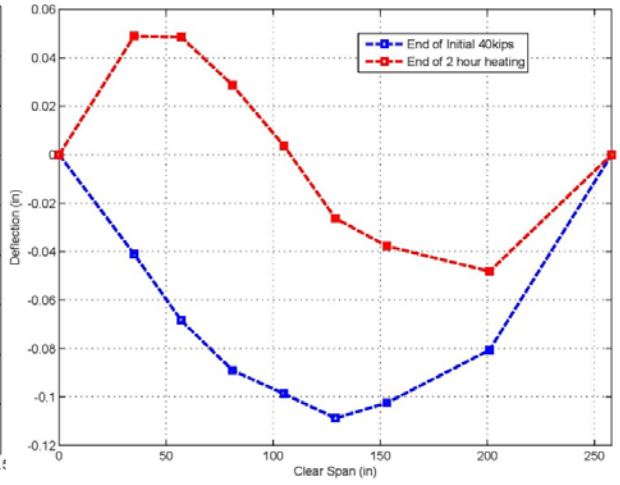

Fig. 5: Typical Temperature History Measured in Spec. 3 **Fig. 6: Deflected Shape Profiles for Specimen 3**

Figure 6 shows the measured deflected shape of Specimen 3 due to the initial loading of 40 kips at each load point, and the final deflected shape after 3 hours of heating, but before the applied loading was increased to failure. As shown the initial loading caused a downward deflection of 0.11 in. The heating applied to the top steel faceplate in the shear span region caused an upward deflection with the maximum value occurring in the center of the heated region (i.e., in the shear span). The peak upward deflection was 0.05 in.

Figure 7 shows the applied load – midspan displacement behavior of Specimen 3 after heating when the loading was increased to failure. For comparison, Figure 7 also includes the applied load –displacement behavior of another specimen that was identical to Specimen 3 but tested without any heating applied. The comparison in Figure 7 shows that thermal loading (applied over only 6 ft length in one the specimen shear spans) does not have a significant influence on the overall strength of the SC beam specimen.

Figure 8 shows the measured moment-curvature response of Specimen 3 in the midspan region away from the applied heating. For comparison, Figure 8 also includes the measured moment-curvature response of the

equivalent specimen that was not subjected to any heating, and the calculated cracked-transformed section flexural stiffness ($EI_{cr\text{-}tr}$). The comparison in Figure 8 shows that the flexural section stiffness away from the region of heating can be predicted reasonably using cracked transformed section properties.

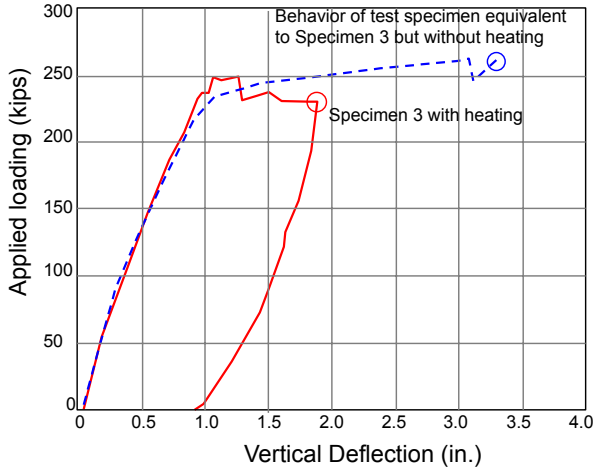

Fig. 7. Load – displacement behavior of Specimen 3

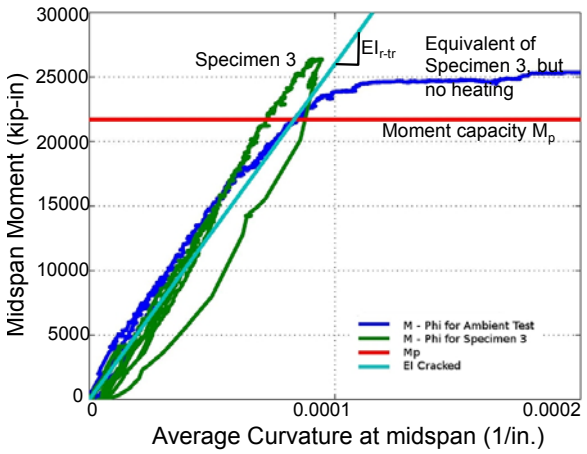

Fig. 8. Moment-curvature behavior of Specimen 3 away from heating

Figure 9 shows the measured average moment-curvature (M-ϕ) response for Specimen 3 at the center of the heated region. The average curvature was estimated by measuring the rotations (θ_1 and θ_2) at each end of the heated region (6 ft apart), and then calculating the average curvature using the central difference equation [(θ_1- θ_2)/ 72 in.]. The figure shows that the thermal gradient through the specimen cross-section causes the section M-ϕ response to shift to the left with negative or upwards curvature (ϕ_{th}) for zero moment. The initial slope of the M-ϕ response is reasonably predicted by the flexural stiffness of the steel section alone (E_sI_s) without any concrete contribution, i.e., assuming fully cracked section. Thus, the bending moment (M_{th}) corresponding to the condition of full rotational restraint (i.e., zero curvature) can be calculated as the product of the steel section flexural stiffness (E_sI_s) and ϕ_{th}.

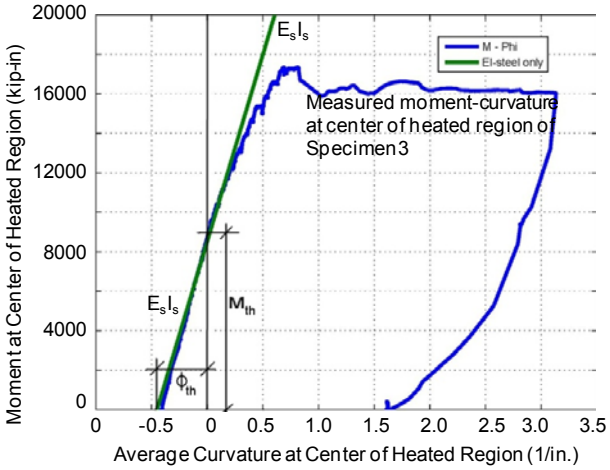

Fig. 9: Average Moment-Curvature Response for Specimen 3 at center of Heated Region

Earlier analytical research conducted by the authors [3, 4, and 5] had shown similar M-ϕ behavior for the heated region of SC beam specimens. The authors had also developed and recommended Equation (1a) for computing $\phi_{th.}$ In Equation 1a, α_s is the thermal expansion coefficient for steel, ΔT_s is the temperature increase for the steel faceplate, T is the section thickness, and t_p is the plate thickness. For Specimen 3, the value of ϕ_{th} calculated using Equation 1a is 5 x 10^{-5} /in. As shown in Figure 9, it compares very well with the experimental value of ϕ_{th}. Thus, Figure 9 and the experimental results for Specimen 3 confirm the analytical research conducted earlier by the authors, and verify the simple equations developed for computing ϕ_{th} and M_{th}, which is the maximum

moment corresponding to full rotational restraint and can be calculated using Equation 1b.

$$\phi_{th} = \frac{\alpha_s \times \Delta T_s}{(T - t_p)} \quad \text{Equation (1a)}$$

$$M_{th} = E_s I_s \; x \; \phi_{th} \quad \text{Equation (1b)}$$

SC WALL: FLEXURAL STIFFNESS

As explained earlier by the authors [3, 4, 5], and further verified here in Figure 8, the flexural stiffness of SC walls not subjected to accident thermal loading can be estimated using cracked-transformed composite section properties ($EI_{cr\text{-}tr}$). The uncracked composite flexural stiffness is generally not manifest in SC walls because of locked in shrinkage strains in the concrete core, and the nature of the mechanical bond (or connection) between the steel plates and the concrete.

The cracked-transformed flexural section stiffness ($EI_{cr\text{-}tr}$) can be estimated using the strain, stress, and force block shown in Figure 10. In Figure 10, n is the concrete-to-steel modular ratio (E_c/E_s), T is the overall section depth, c is the distance to the neutral axis, and t_p is the plate thickness. The uncracked concrete (in compression) is transformed into equivalent steel using the modular ratio (n). Strain compatibility is assumed, and the top plate strain is assumed to be equal to ε_c. Solving the force equilibrium equation results in Equation 2 for the neutral axis depth, wherein ρ' is the stiffness normalized reinforcement ratio that can be calculated using Equation 3. The cracked-transformed flexural stiffness can then be computed using Equation 4.

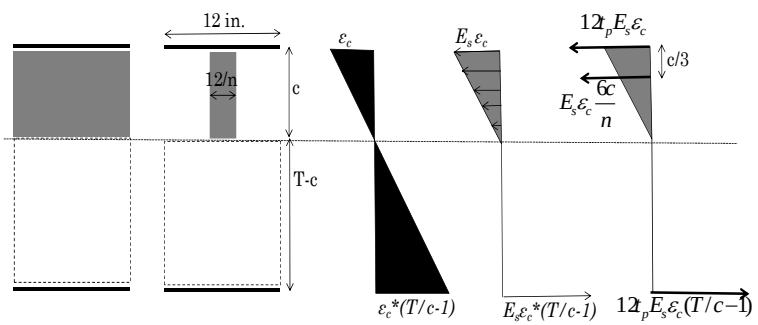

(a) cracked section, (b) transformed, (c) strain profile, (d) stress profile, (e) force profile

Fig. 10. Flexural stiffness of cracked-transformed section of SC walls.

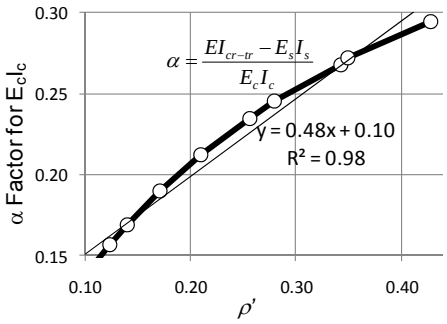

Fig. 11 Calibration of Eq. 5

$$\frac{c}{T} = \sqrt{\rho'^2 + \rho'} - \rho' \quad \text{(Equation 2)}$$

Where,
$$\rho' = \frac{2t_p}{T}\frac{E_s}{E_c} \quad \text{(Equation 3)}$$

$$EI_{cr\text{-}tr} = E_s\left[12t_pT^2\left[1 + 2\left(\frac{c}{T}\right)^2 - 2\frac{c}{T} - \frac{t_p}{T}\right] + \frac{4T^3}{n}\left(\frac{c - t_p}{T}\right)^3\right] \quad \text{(Equation 4)}$$

Equation 4 is accurate but reasonably complex. It was calibrated to the simpler form given by Equation 5, which separates the contribution of the steel and concrete parts, and uses a reduction factor (α) to account for concrete cracking. In Equation 5, I_c is the moment of inertia contribution of the total concrete infill. The calibration of Equation (5) to $EI_{cr\text{-}tr}$ is shown graphically in Figure 11. As shown the calibration resulted in Equation 6 for estimating the alpha-factor (α) as a function of the stiffness normalized reinforcement ratio (ρ').

$$EI_{cr\text{-}tr} = E_sI_s + \alpha E_cI_c \quad \text{(Equation 5)}$$

Where, $\alpha = 0.48\,\rho' + 0.10$ (Equation 6)

SC walls subjected to operating or ambient thermal conditions (T_o) generally develop steady-state linear thermal gradients through the cross-section due to the slow rate of thermal loading and the large thermal inertia of concrete. Since the thermal gradients are linear, there is no significant additional cracking of the composite section besides that due to the applied loading. As a result, the flexural stiffness calculated using Equations 5 and 6 can be used for loading combinations involving operating thermal conditions.

As explained earlier by the authors [3, 4, 5], and further verified here in Figure 9, the flexural stiffness of SC walls subjected to accident thermal loading (T_a) can be estimated using fully-cracked section properties (E_sI_s) of the composite section.

Based on this discussion, an effective flexural stiffness (EI_{eff}) equation (Equation 7) is proposed for the out-of-plane flexural stiffness of SC walls that takes into account the reduction of stiffness due to concrete cracking and thermal effects. This equation assumes a linear reduction in flexural stiffness from $EI_{cr\text{-}tr}$ (Equation 5) to E_sI_s for temperature change (ΔT_s) from 0 to 150°F. ΔT_s corresponds to the maximum temperature increase in the steel faceplates, and ΔT_s of 150°F corresponds to a thermal strain of about $1x10^{-4}$ (assuming steel thermal expansion coefficient of about 6.5 x 10^{-6} /°F), which is approximately the cracking strain for concrete.

$$EI_{eff} = \left(E_sI_s + \alpha E_cI_c\right)\left(1 - \frac{\Delta T_s}{150F}\right) \geq E_sI_s \qquad \text{(Equation 7)}$$

For ΔT_s greater than 150°F, the flexural stiffness is limited to that of the steel alone, i.e., fully cracked section. It is important to note that accident thermal loads are typically in the range of about 300°F, which is low enough to only cause a negligible impact on steel material properties. It is reasonable to use the same steel properties for both non-accident and accident conditions.

SC WALL: IN-PLANE SHEAR STIFFNESS

As explained above, operating thermal conditions are not expected to develop significant additional cracking in the concrete. The in-plane shear stiffness for loading combinations involving operating thermal conditions can be estimated according to the general in-plane stiffness of SC walls, which has been studied extensively in Japan. Ozaki et al. [6] and Varma et al. [7] have discussed the basic mechanics of in-plane shear behavior in SC walls. They have developed a tri-linear shear force-shear strain (S_{xy}-γ_{xy}) model for SC walls that is shown in Figure 12 along with the equations needed to construct this tri-linear model for SC walls with reinforcement ratios ($2t_p/T$) from 1.5-5%. In Figure 12, E_s, ν_s, G_s, A_s, F_y are the elastic modulus, poisson ratio, shear modulus, area, and yield stress of the steel plates. E_c, G_c, A_c, and f'_c are the elastic modulus, shear modulus, area, and compressive strength in psi of the concrete.

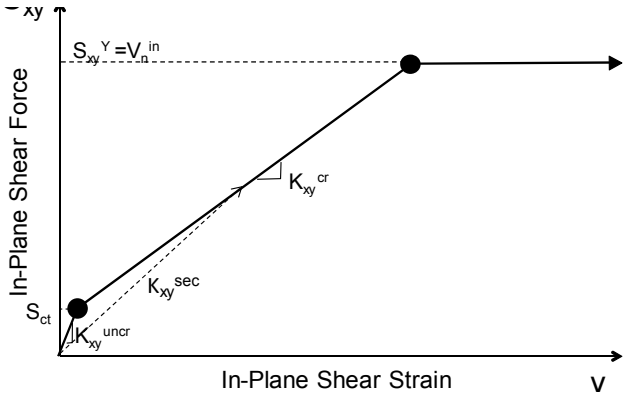

$$K_{xy}^{uncr} = G_sA_s + G_cA_c$$

$$S_{ct} = \left(\frac{0.002\sqrt{f'_c}}{E_c}\right)\left(E_cA_c + E_sA_s\right)$$

$$S_{xy} = (K_{xy}^{cr})\,\gamma_{xy} = \left(K_s + K_{sc}\right)\gamma_{xy}$$

$$S_{xy}^{Y} = V_n^{in} = \frac{K_s + K_{sc}}{\sqrt{3K_s^2 + K_{sc}^2}} \times A_sF_y$$

$$where, K_s = G_sA_s$$

$$and, K_{sc} = \frac{1}{\frac{4}{0.7E_cA_c} + \frac{2(1-\nu_s)}{E_sA_s}}$$

Fig. 12. In-plane Shear Behavior of SC Walls

The first branch in Figure 12 corresponds to the uncracked composite behavior of the SC wall. The initial stiffness (K_{xy}^{uncr}) before concrete cracking is governed by shear stiffness of the steel-concrete composite section. Concrete cracking occurs when the applied shear exceeds the cracking threshold (S_{ct}), which corresponds to a concrete principal stress of $2(f'_c)^{0.5}$ in psi. The concrete cracking threshold is reduced [from potentially from $4(f'_c)^{0.5}$] by the locked in shrinkage strains in the concrete, which is similar to their influence on the flexural response discussed earlier. The second branch corresponds to the cracked composite behavior of the SC wall. The tangent stiffness (K_{xy}^{cr}) after cracking is governed by the cracked orthotropic behavior of the concrete acting composite with steel plates that are in a state of plane stress. Steel plate yielding occurs when the applied shear reaches S_{xy}^{Y}, which causes Von Mises yielding of the steel plate due to the stresses induced in it. The third branch corresponds to the plastic behavior of the SC wall after steel plate Von Mises yielding.

Under seismic loading conditions, the cyclic behavior of SC walls is governed by the secant stiffness (K_{xy}^{sec} identified in Figure 12) not the tangent stiffness. Figure 13 shows the variation of $K_{xy}^{sec}/K_{xy}^{uncr}$ with respect to S_{xy}/S_{xy}^{Y}. As shown, the secant stiffness drops exponentially after cracking occurs, and stabilizes to reach the post-cracking stiffness (K_{xy}^{cr}) asymptotically.

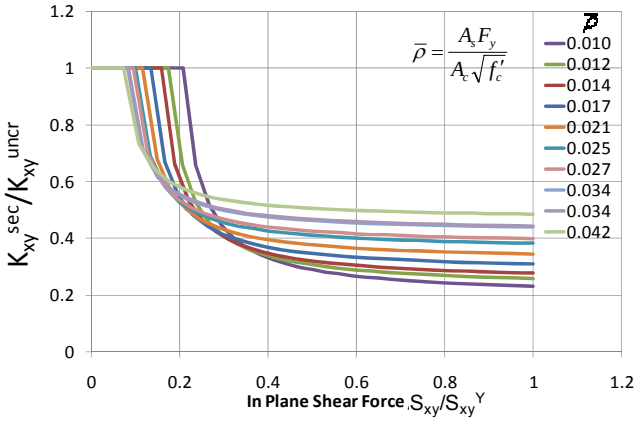

Fig. 13 Secant stiffness of SC walls

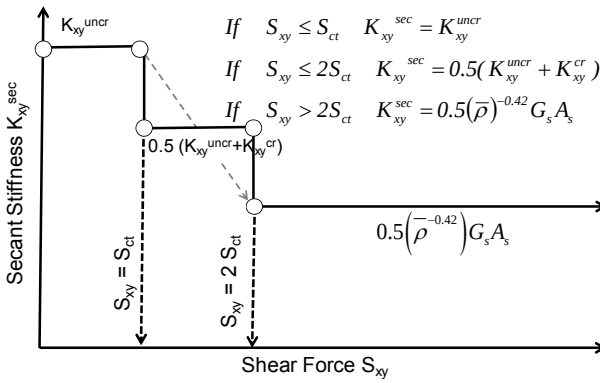

Fig. 14. Model for Estimating Secant Stiffness of SC Walls

Figure 14 shows a simple three-step model that was developed by the authors to capture the secant stiffness variation with the applied shear force As shown, when S_{xy} is less than the cracking threshold (S_{ct}), the secant stiffness (K_{xy}^{sec}) can be assumed to be equal to K_{xy}^{uncr}. When S_{xy} is greater than S_{ct} but less than $2S_{ct}$, K_{xy}^{sec} can be assumed to be the average of K_{xy}^{uncr} and the cracked shear stiffness (K_{xy}^{cr}). When S_{xy} is greater than $2S_{ct}$, K_{xy}^{sec} can be assumed according to Equation (8), wherein $\bar{\rho}$ is a strength normalized reinforcement ratio calculated as $A_sF_y/A_c(f'_c)^{0.5}$. More accuracy can be obtained by using a linear interpolation between S_{ct} and $2S_{ct}$ instead of the stepped approach (also shown in Figure 14). This model reasonably predicts the calculated secant stiffness of SC walls with reinforcement ratios of 1.5-5%, concrete f'_c from 4000-6000 psi, and steel F_y from 36 to 65 ksi. The actual comparisons could not be included here for length reasons.

$$If\ S_{xy} > 2S_{ct};\quad K_{xy}^{sec} = 0.5(\bar{\rho})^{-0.42} G_s A_s \qquad \text{Equation (8)}$$

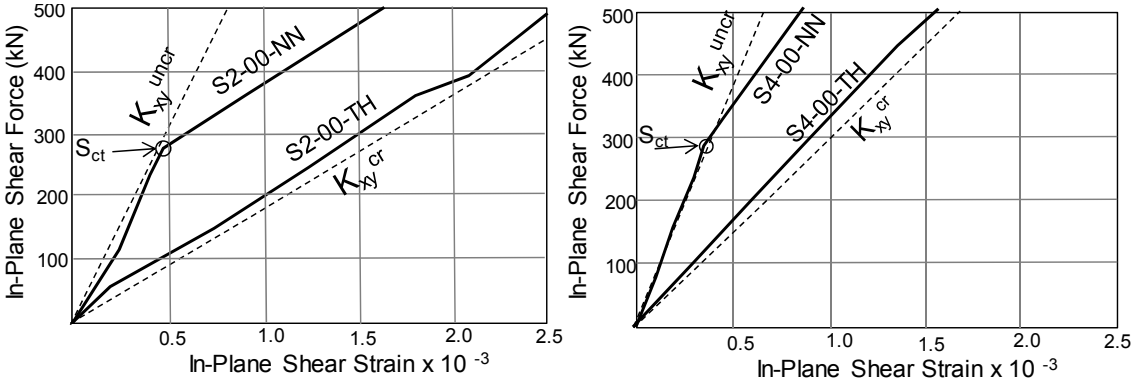

Fig. 15. Initial Portion of In-Plane Shear Force vs. Shear Strain of Specimens Tested by Ozaki et al. [8]

Ozaki et al. [8] have experimentally investigated the effects of accident thermal loading on the in-plane shear behavior of SC walls. They subjected SC wall specimens (with reinforcement ratios from 2.3 – 4.5%) to accident thermal loading in the form of heating applied to both steel faceplates from the outside. The faceplates were heated from ambient temperature to 375°F at the rate of 104°F/hour. The steel temperature was maintained at 375°F for 24 hours, after which natural cooling was allowed to occur. After cooling, the specimens were subjected to cyclic in-plane shear loading. Identical specimens without any heating were also tested for comparison [6].

The experimental results indicate that accident thermal loading develops nonlinear (parabolic) thermal gradients through the concrete section. This nonlinear gradient produces orthogonal crack patterns in the concrete because of the continuum nature and expansion of the steel faceplates. These orthogonal cracks affect the in-plane shear stiffness of the SC walls but not the strength [8]. Figure 15 shows comparisons of the initial portion of the in-plane shear force-shear strain response of SC wall specimens tested with and without thermal loading effects. In this figure, S2-00-TH and S4-00-TH are specimens (with reinforcement ratios of 2.3 and 4.5%) that were exposed to thermal cracking first. Specimens S2-00-NN and S4-00-NN were tested without thermal loading. The comparisons show that accident thermal loading eliminates the first (uncracked) branch of shear force- strain behavior.

CONCLUSIONS AND RECOMMENDATIONS FOR ANALYSIS

The design loading combinations for nuclear structures [9] include: (i) seismic + operating thermal (T_o), and (ii) seismic + accident thermal (T_a) loading conditions. Operating (and ambient) thermal conditions produce gradual temperature changes and approximately linear temperature gradients through the section depth. They do not cause significant additional cracking besides that caused by the seismic loading itself. On the other hand, accident thermal conditions cause rapid temperature changes, and produce nonlinear temperature gradients through the section depth causing significant additional concrete cracking.

Experimental and analytical research shows that in the absence of accident thermal loading the flexural stiffness of SC composite walls can be estimated using cracked-transformed section properties (Equation 5). In the presence of accident thermal loading, the flexural stiffness reduces significantly to that of the steel section alone. Equation 7 provides a simple model to estimate the reduced flexural stiffness of SC walls.

In the absence of accident thermal loading, the in-plane shear stiffness of SC walls can be estimated as the secant stiffness provided by the model shown in Figure 14. Since the secant stiffness depends on the applied in-plane shear loading (S_{xy}), some iteration may be needed to finalize the secant stiffness of the SC walls. In the presence of accident thermal loading, the in-plane shear stiffness reduces significantly to the post-cracking value that can be estimated approximately using Equation 8.

Nuclear power plant structures are generally analyzed using finite element models with linear elastic material properties due to the limitations of soil-structure interaction (SSI) analysis programs and methods. These linear elastic finite element (LEFE) models for SC walls should be calibrated to model the flexural and in-plane shear stiffness outlined in this paper and summarized above. Since, the SC composite walls will typically be modeled using one hypothetical linear elastic material with elastic modulus (E_m) and poisson ratio (ν_m); the poisson ratio can be assumed to that of the concrete, and the elastic modulus (E_m) and wall section thickness (T_m) can be calibrated to model the appropriate flexural and in-plane shear stiffness outlined in this paper.

It is important to note that two different LEFE models will be needed, one to match the stiffness characteristics of seismic + T_o condition, and the second to match the stiffness characteristic of seismic + T_a condition. The results from the LEFE SSI analyses will be used to estimate the demands for analyses. As shown in the paper, flexural moments induced by accident thermal loading conditions at locations away from supports or restraints need not exceed the value M_{th} calculated using Equation 1b.

ACKNOWLEDGMENTS

The research presented in this paper was partially funded by Bechtel Corp. and also partially funded by Westinghouse Electric Corp. All findings presented in the paper are strictly those of the authors.

REFERENCES

[1] MPR-2610 Revision 2. “Application of Advanced Construction Technologies to New Nuclear Power Plants”, Dept. of Energy Report, Sep. 2004, http://www.ne.doe.gov/np2010/reports/mpr2610Rev2Final924.pdf

[2] Adams, P. F., Zimmerman, T. J. E., and MacGregor, J.G. (1988), “Design and Behavior of Composite Ice-Resisting Walls.” *ACI Special Pub. SP109-20*, ACI, Farmington Hills, MI.

[3] Booth, P.N. “Behavior of Steel Plate Reinforced Concrete Modular Walls Subjected to Combined Thermal and Mechanical Loads.” *M.S. Thesis*, Purdue University, School of Civil Eng., West Lafayette, IN 47906

[4] Booth, P.N., Varma, A. H., Malushte, S. R., Johnson, W. H., “Response of Modular Composite Walls to Combined Thermal & Mechanical Load.” *Trans. of the Internal Assoc. for Struct. Mech. in Reactor Tech. Conf.*,, *SMiRT-19, Paper No. H01/4.*Toronto, Canada, Aug. 2007, 10 pp.

[5] Varma, A.H., Malushte, S.R., Sener, K.C., and Booth, P.N. (2009). “Analysis and Design of Modular Composite Walls for Combined Thermal and Mechanical Loading.” *Trans. of the Internal Assoc. for Struct. Mech. in Reactor Tech. Conf., SMiRT-20, Div. TS 6 Paper 1820*, Espoo, Finland, Aug. 9-14, 2009.

[6] Ozaki, M., Akita, S., Oosuga, H., Nakayama, T., Adachi, N. (2004). “Study on Steel Plate Reinforced Concrete Panels Subjected to Cyclic In-Plane Shear.” *Nuclear Engg. and Design*, Vol. 228, pp. 225-244.

[7] Varma, A.H., Zhang, K., Chi, H., Booth, P.N., and Baker, T. (2011). “In-Plane Shear Behavior of SC Walls: Theory Vs. Experiment.” *Trans. of the Internal Assoc. for Struct. Mech. in Reactor Tech. Conf., SMiRT-21, Paper No. 764*, New Delhi, India, Nov. 6-11, 2011.

[8] Ozaki, M., Akita, S., Takeuchi, M., Oosuga, H., Nakayama, T., and Niwa, H., (2000). "Experimental Study on Steel-plate-reinforced Concrete Structure Part 41: Heating Tests (Outline of Experimental Program and Results), Annual Conference of Architectural Institute of Japan, 2000, Part 41-43, pp. 1127-1132.

[9] ACI 349-06 (2006). *Code Reqs. for Nuclear Safety Related Conc. Struct. and Comm.* ACI, Farmington Hills, MI